Published in final edited form as:
Nature. 2009 July 2; 460(7251): 103–107. doi:10.1038/nature08097.

Enhancing CD8 T Cell Memory by Modulating Fatty Acid Metabolism

Erika L. Pearce[1], **Matthew C. Walsh**[1], **Pedro J. Cejas**[1], **Gretchen M. Harms**[1], **Hao Shen**[2], **Li-San Wang**[1,3], **Russell G. Jones**[4], and **Yongwon Choi**[1]

[1]Department of Pathology and Laboratory Medicine, University of Pennsylvania School of Medicine, Philadelphia, PA 19104, USA

[2]Department of Microbiology, University of Pennsylvania School of Medicine, Philadelphia, PA 19104, USA

[3]Penn Center for Bioinformatics, University of Pennsylvania School of Medicine, Philadelphia, PA 19104, USA

[4]McGill Cancer Centre, Department of Physiology, McGill University, Montreal, QC, H3G 1Y6, CANADA

Abstract

CD8 T cells, which play a crucial role in immunity to infection and cancer, are maintained in constant numbers, but upon antigen stimulation undergo a developmental program characterized by distinct phases encompassing the expansion and then contraction of antigen-specific effector (T_E) populations, followed by the persistence of long-lived memory (T_M) cells[1, 2]. Although this predictable pattern of CD8 T cell responses is well established, the underlying cellular mechanisms regulating the transition to T_M remain undefined1, [2]. Here we show that TRAF6, an adapter protein in the TNF-receptor (TNFR) and IL-1R/TLR superfamily, regulates CD8 T_M development following infection by modulating fatty acid metabolism. We show that mice with a T cell-specific deletion of TRAF6 mount robust CD8 T_E responses, but have a profound defect in their ability to generate T_M that is characterized by the disappearance of antigen-specific cells in the weeks following primary immunization. Microarray analyses revealed that TRAF6-deficient CD8 T cells exhibit altered expression of genes that regulate fatty acid metabolism. Consistent with this, activated CD8 T cells lacking TRAF6 display defective AMPK-activation and mitochondrial fatty acid oxidation (FAO) in response to growth factor withdrawal. Administration of the anti-diabetic drug metformin restored FAO and CD8 T_M generation in the absence of TRAF6. Remarkably, this treatment also increased CD8 T_M in wild type mice, and consequently was able to significantly improve the efficacy of an experimental anti-cancer vaccine.

A prevailing paradigm in immunology is that antigenic signal strength drives progressive T cell differentiation [3]. To investigate this model regarding T_M, we studied CD8 T cell responses to bacterial infection in mice with a T cell-specific deletion of TRAF6 (TRAF6-ΔT), a negative regulator of antigen-specific T cell activation [4]. Despite having fewer total CD8 T cells (SI Fig. 1), TRAF6-ΔT mice mounted normal Ova-specific T_E responses to attenuated *L. monocytogenes* expressing Ova (LmOva) (Fig. 1a and SI Fig. 2). To examine CD8 T_M in TRAF6-ΔT mice, we immunized with LmOva and measured Ova-specific cells 60 days post-infection. Although Ova-specific T_E responses were intact, CD8 T_M generation in TRAF6-

Correspondence to: Yongwon Choi (ychoi3@mail.med.upenn.edu).

Microarray data is in the public repository Gene Expression Omnibus (GEO) and the accession number is GSE15750.

ΔT mice was severely compromised (Fig. 1b and SI Fig. 3), even with 10-fold higher or lower immunizing doses (not shown). In mice lacking *cbl-b* [5], a different negative regulator of antigen-specific T cell activation, T_M developed normally (SI Fig. 4), indicating that failure of T_M generation in TRAF6-ΔT mice cannot be entirely explained by loss of a negative regulator.

A hallmark of T_M is the ability to mount accelerated recall responses to challenge infection. To confirm the impaired generation of CD8 T_M in TRAF6-ΔT mice, we challenged previously immunized CTRL and TRAF6-ΔT mice with LmOva and measured Ova-specific cells 7 days later. TRAF6-ΔT mice failed to respond robustly to re-infection, suggesting that T_M may not have been generated and that the smaller Ova-specific population present in TRAF6-ΔT mice was a new primary response (Fig. 1c). To determine if TRAF6-ΔT mice generate T_M, we transferred equal numbers of Ova-specific cells from previously immunized CTRL and TRAF6-ΔT mice 28 days post-infection, at which time a small population of Ova-specific cells appeared to be present (SI Fig. 3), and compared functionality on a per cell basis in response to challenge. We reasoned that naïve donor cells transferred into immune-competent animals would not respond to infection because they would be vigorously outcompeted by endogenous naïve cells, and only T_M donor cells would mount accelerated recall responses that could outcompete endogenous naïve cells. At day 7 post-challenge, donor-derived Ova-specific secondary T_E cells from CTRL mice represented 11% of the engrafted population while TRAF6-ΔT donor cells were undetectable (SI Fig. 5), demonstrating a severe impairment in CD8 T_M development in TRAF6-ΔT mice.

TRAF6-ΔT mice accumulate CD4 T cells and develop multi-organ inflammatory disease [4]. Since CD4 T cells can influence CD8 T cells responses [6–8] we wanted to rule out effects from the TRAF6-deficient CD4 T cell compartment. To determine if defective CD8 T_M generation in TRAF6-ΔT mice was intrinsic to CD8 T cells, we crossed TRAF6-ΔT mice with MHCI-restricted Ova-specific TCR-transgenic OT-I mice. Since OT-I mice lack CD4 T cells, generating OTI-TRAF6-ΔT mice allowed us to assay a pure population of uniformly naïve TRAF6-deficient CD8 T cells (SI Figs. 6–8). We transferred OTI-TRAF6-WT and OTI-TRAF6-ΔT cells into congenic recipients, which possess a normal CD4 T cell compartment, and then immunized with LmOva (Fig. 2a). By transferring only small numbers of transgenic cells we could measure endogenous Ova-specific cells at the same time as the engrafted donor response, allowing us to assume that the majority of donor cells were activated [9]. In addition, following T cell responses by serially bleeding allowed us to compare the kinetics of responding CD8 T cells within individual animals. Although both OTI-TRAF6-WT and OTI-TRAF6-ΔT donor cells mounted strong T_E responses (days 4–6), OTI-TRAF6-ΔT cells were not maintained during contraction (days 10–21) and were undetectable by 3 weeks post-infection (Fig. 2b,c and SI Fig. 9). Donor T_E cells from both genotypes exhibited similar expression of classical activation markers following primary immunization (SI Figs. 10,11) however, consistent with published data regarding killer cell lectin-like receptor 1 (KLRG1) as a marker for short-lived T_E cells that do not form T_M, a greater percentage of the OTI-TRAF6-ΔT T_E population expressed higher levels of KLRG1 (SI Fig. 12) [10]. Following challenge infection, only donor OTI-TRAF6-WT T_M cells responded robustly (Fig. 2b,c and SI Fig. 9). These results demonstrate that although TRAF6 is dispensable for CD8 T_E responses, TRAF6 signaling within CD8 T cells is crucial to T_M generation.

Antigen-specific CD8 T cells responding to infection are not a homogenous population, but consist of small numbers of T_M precursors that express IL-7Rα [11]. In conjunction with this idea, numerous studies have delineated roles for the γ_c cytokines IL-7 and IL-15 as critical factors for CD8 T cell homeostasis and T_M development [12–15]. Impaired γ_c cytokine signaling in TRAF6-deficient CD8 T cells could explain the defect in their ability to form T_M. We tested the ability of CD8 T_E cells to respond to IL-15 and found that both OTI-TRAF6-WT and OTI-

TRAF6-ΔT cells exhibit similar responsiveness to this cytokine (SI Fig. 13,14). To be sure that the lack of T_M development by TRAF-6-deficient CD8 T cells is not secondary to a defect in survival, and to further investigate a possible defect in γ_c cytokine signaling, we crossed OTI-TRAF6-ΔT mice to mice constitutively expressing an active form of Stat-5 (CA-St5) [16], a critical γ_c cytokine receptor downstream signaling molecule [16]. CD8 T cells expressing CA-St5 show augmented survival, proliferation, and Bcl-2 expression [17], and CA-St5 mice exhibit selective expansion of memory-like CD8 T cells [16]. We transferred CA-St5-OTI-TRAF6-WT and CA-St5-OTI-TRAF6-ΔT cells into congenic mice, immunized, and followed the donor and host Ova-specific responses (Fig. 2d and SI Fig. 15). Contraction of CA-St5-OTI-TRAF6-WT populations was reduced compared to control OT-I populations (Figs. 2c and 2d). Surprisingly however, CA-St5-OTI-TRAF6-ΔT cells were not rescued from contracting to undetectable levels 3 weeks post-infection (Fig. 2d and SI Fig. 15). Importantly, we confirmed that CA-St5 expression in TRAF6-deficient CD8 T cells enhanced survival in an *ex vivo* survival assay (SI Fig. 16), suggesting that the severe contraction exhibited by the TRAF6-deficient OT-I population (Fig. 2c,d and SI Fig. 15) and the ensuing lack of T_M development is not secondary to a general survival defect. Animals primed with the challenge dose of bacteria 3 weeks post-transfer showed no differences in the T_E response between the genotypes (Fig. 2e and SI Fig. 15), indicating that the loss of TRAF6-deficient CD8 T cells is exaggerated in response to signals following infection, and not simply due to defects in homeostatic signals following transfer.

We used a systems biology approach to identify unique gene expression signatures between OTI-TRAF6-WT and OTI-TRAF6-ΔT CD8 T cells that could account for their differences in survival following infection. We performed microarray analyses for both genotypes 6 and 10 days post-transfer and infection (SI Fig. 17). Due to similar survival rates between OTI-TRAF6-WT and OTI-TRAF6-ΔT CD8 T cells during the peak of the T_E response, but striking differences in survival during contraction, we reasoned that expression of genes related to survival might begin to diverge between genotypes at d10 post-infection. We used the NIAID DAVID website to look for pathways in the KEGG database that have significant overlaps with differentially expressed genes in our microarray experiment. We discovered that TRAF6-deficient cells from d10 post-infection displayed defects in the expression of genes which function in several metabolic pathways, including fatty acid metabolism (Fig. 3a).

FAO is an important survival pathway in metabolically stressed cells [18] and the removal of signals associated with infection, such as growth factor cytokines including IL-2, induces metabolic stress in hematopoietic cells [19, 20]. Therefore, we tested the ability of OTI-TRAF6-WT and OTI-TRAF6-ΔT CD8 T cells to oxidize fatty acids following withdrawal of the pro-proliferative growth factor cytokine IL-2 *in vitro*. After IL-2 withdrawal, only control OTI-TRAF6-WT CD8 T cells increased FAO to a high degree (Fig. 3b). Consistent with normal activation (SI Fig. 18), activated control and TRAF6-deficient CD8 T cells increased glycolysis in response to IL-2 (data not shown). Also, TRAF6-deficient CD8 T cells displayed normal upregulation of FAO in response to glucose withdrawal, indicating that cells are not completely unfit in the absence of TRAF6, but rather their inability to regulate catabolic fatty acid metabolism is due to the lack of a specific signal from growth factor (SI Fig. 19). Importantly, although transgenic-expression of CA-St5 did enhance T cell survival following infection (SI Fig. 16), it did not rescue the defect in FAO in TRAF6-deficient cells following growth factor withdrawal (SI Fig. 20), suggesting that FAO defects are not secondary to survival defects.

Proliferating T cells use glycolytic metabolism rather than FAO for energy generation [21–23], and growth factors enable this bias [24]. In the absence of glucose, cells can survive in part by ceasing proliferation and switching to catabolic metabolism like FAO and autophagy [18, 20]. OTI-TRAF6-ΔT CD8 T cells were notably less capable of effecting this metabolic switch than OTI-TRAF6-WT CD8 T cells following IL-2 withdrawal (Fig. 3c). This suggested that

TRAF6-deficient CD8 T cells responding to infection are unable to survive contraction and persist as long-lived T_M due to an inability to properly engage pathways of FAO when growth factors like IL-2 become limiting after the peak of the immune response.

AMP-activated kinase (AMPK) and Akt are central regulators of FAO and glycolyis, respectively [23]. Consistent with reduced FAO, TRAF6-deficient CD8 T cells have lower active AMPK levels following IL-2 withdrawal (Fig. 3d). To investigate whether AMPK defects could underlie decreased FAO in TRAF6-deficient CD8 T cells, we measured the effect of the anti-diabetic drug metformin, which promotes AMPK activation [25], on FAO following IL-2 withdrawal. Metformin increased AMPK activation (Fig. 3d) and rescued FAO in TRAF6-deficient CD8 T cells (Fig. 3e). In contrast, FAO in TRAF6-deficient cells was unaffected by the Akt inhibitor triciribine (Fig. 3e), suggesting that Akt may not regulate this metabolic pathway. These data support that FAO initiation following the peak of infection, accompanied by the reduction in T cell survival signals, underlies T_M development, and that commitment to this metabolic pathway is affected when TRAF6 is absent. In such a case, stimulating FAO in TRAF6-deficient CD8 T cells would rescue the observed defects and promote T_M. Consistent with this hypothesis, OTI-TRAF6-ΔT CD8 T cells had lower levels of active AMPK at the peak of the T_E response (Fig. 3f).

To explore if inducing FAO *in vivo* would rescue the observed defects in TRAF6-deficient CD8 T cells and promote T_M, we administered metformin daily following T cell transfer and infection. Remarkably, metformin not only promoted survival of OTI-TRAF6-ΔT CD8 T cells throughout contraction, but also of endogenous Ova-specific cells, resulting in enhanced T_M with the capacity to respond to re-infection (Fig. 4a and SI Fig. 21). Metformin also promoted OTI-TRAF6-WT CD8 T cell survival (Fig. 4b). Treatment with a second FAO-inducing drug [26–28], the mTOR (mammalian target of rapamycin) inhibitor rapamycin, resulted in strikingly increased T_M development and ensuing recall response for both OTI-TRAF6-ΔT and OTI-TRAF6-WT CD8 T cells (Fig. 4a,b and SI Fig. 21). Together these data strongly point towards the commitment to FAO as a key requirement for T_M development, and the pharmacological modulation of this metabolic pathway as a potential target for vaccine design.

Promoting CD8 T_M development is a major goal of vaccination. Our data showing increased CD8 T_M for donor OT-I and endogenous Ova-specific cells following metformin treatment suggested that commitment to FAO is generally important for CD8 T_M development, and not only in settings of TRAF6-deficiency. This led us to the idea that pharmacological modulation of T cell metabolism could enhance vaccine efficacy. To test this we utilized an experimental vaccine against an aggressive tumor [29]. We immunized control mice with LmOva and then began daily injections of PBS or metformin following the peak of the T_E response. After three weeks, drug treatment ceased and mice were inoculated with EL4-Ova tumor cells (Fig. 4c). Metformin was administered after T_E cell expansion to avoid the possibility of altering the T_E response. To rule out direct effects of metformin on tumor growth, treatment was stopped 24 hours before tumor injection. Following EL4-Ova inoculation, 6/9 metformin-treated mice survived >33 days compared to only 1/8 PBS-treated mice (Fig. 4c). This increase in survival following metformin treatment correlated with an increase in T_M cells prior to tumor inoculation (SI Fig. 22), suggesting that metformin treatment enhanced T_M cell generation resulting in greater protective anti-tumor immunity.

Proliferating T cells utilize glucose as their main energy source and suppress fatty acid metabolism, while quiescent cells (i.e. naïve and T_M) break down fatty acids, amino acids, and glucose interchangeably for energy [23]. As such, proliferating T_E cells display an anabolic signature typified by increased glycolytic metabolism, while T_M cells display a catabolic signature. This implies that during contraction there is an active conversion of cellular energy metabolism in order to generate T_M. Current models suggest that during contraction T cells

compete for growth factors such as IL-2, and we speculate that as these growth factors become limiting, cells become stressed and undergo a metabolic transformation essential for T_M generation. We propose a model where TRAF6 plays a critical role following infection by regulating a metabolic switch in CD8 T cells that promotes survival and development into long-lived T_M.

Investigating the role of TRAF6 in T_M development led us to the surprising finding that energy metabolism can be pharmacologically manipulated during an immune response to promote CD8 T_M generation and protective immunity. Although the exact mechanism of metformin-mediated CD8 T_M enhancement remains unclear, our work suggests that metabolism-altering drugs hold promise as immunotherapeutics and command further study as modulators of T cell responses. Metformin has been shown to inhibit tumor progression [25, 30], although given our results it is unclear how metformin-regulated changes in T_M contribute to its anti-tumor properties. Our findings highlight a critical link between metabolic transitions and cell fate determination, and may have important implications for therapeutic and prophylactic vaccine development.

Methods Summary

TRAF6$^{flx/flx}$CD4-cre(−) (CTRL) and TRAF6$^{flx/flx}$CD4-cre(+) (TRAF6-ΔT) were bred in house (backcrossed >10 generations to C57BL/6) and have been previously described [4]. C57BL/6 (WT) and OT-I transgenic mice were purchased from The Jackson Laboratory (Bar Harbor, ME). OT-I mice were bred to TRAF6$^{flx/flx}$CD4-cre mice to generate control OT-I-TRAF6$^{flx/flx}$CD4-cre(−) or OT-I-TRAF6$^{flx/+}$CD4-cre(+) mice (OTI-TRAF6-WT) and OT-I-TRAF6$^{flx/flx}$CD4-cre(+) (OTI-TRAF6-ΔT). Mice expressing the constitutively active Stat5 transgene (CA-St5) [16] were provided by Michael Farrar (University of Minnesota) and bred to OT-I-TRAF6$^{flx/+}$CD4-cre(+) mice to generate control OT-I-CASt5-TRAF6$^{flx/flx}$CD4-cre(−) mice (OTI-CA-St5-TRAF6-WT) and OT-I-CA-St5-TRAF6$^{flx/flx}$CD4-cre(+) mice (OTI-CA-St5-TRAF6-ΔT). Age-matched CTRL and TRAF6-ΔT mice were injected i.v. with a sub-lethal dose of 1×10^6 CFU of recombinant attenuated *L. monocytogenes* (LmOva) for primary immunizations and challenged i.v. with 1×10^7 CFU for secondary immunizations. CD45.1 congenic mice from OT-I adoptive transfer experiments were injected with a sub-lethal dose of 5×10^6 CFU of LmOva for primary immunizations and were challenged i.v. with 5×10^7 CFU for secondary immunizations. Acute LmOva infections are resolved and bacteria are cleared by day 7 in all mice. All p-values were calculated using unpaired two-tailed Student's *t* test.

Methods

Mice

Cbl-b−/− mice were a gift from Josef Penninger. B6.Ly5.2/Cr (CD45.1 congenic) mice were purchased from the National Cancer Institute (Frederick, MD). All animals were cared for according to the Animal Care Guidelines of the University of Pennsylvania.

Immunizations

We used the attenuated strain of rLmOva deleted for *actA* (LmOva) [31] throughout this paper for convention, however, challenging CTRL and TRAF6ΔT mice with 1×10^6 CFU of non-attenuated recombinant *Listeria* expressing Ova [32], or priming and challenging CD45.1 congenic mice from an OT-I adoptive transfer with 1×10^5 CFU and 1×10^6 of recombinant *Listeria* expressing Ova respectively, yielded similar results. To determine bacterial clearance CTRL and TRAF6-ΔT were immunized with 8×10^6 CFU LmOva and colony forming units per spleen and liver were determined 2, 4, and 6 days after infection as described [31]. 5×10^6 EL4-Ova (EG.7) tumor cells were injected into the right flank of mice as indicated.

Flow cytometry and intracellular cytokine staining

All fluorochrome-conjugated monoclonal antibodies were purchased from BD Pharmingen (San Diego, CA) or from eBioscience (San Diego, CA). All staining was performed as previously described [31]. For *ex vivo* intracellular cytokine staining, cells were cultured at 37° C for 5hr in complete medium supplemented with 100U/ml of recombinant human IL-2, 1.0 μl/ml GolgiStop, in either the presence or absence of $Ova_{257–264}$ peptide at 1.0 μg/ml. Ova-specific $CD8^+$ T cells were also quantified by direct staining with H2-K^b/$Ova_{257–264}$ (K^b/Ova) MHC/peptide tetramers, either by sacrificing animals and cells harvested from organs or by collecting blood from a live animal (serial bleeds), as indicated.

Adoptive transfers

Splenocytes from CTRL and TRAF6-ΔT mice 28 days post-immunization were stained with K^b/Ova tetramer to determine numbers of Ova-specific CD8 T cells. Splenocytes containing 1×10^4 of Ova-specific cells were transferred intravenously to recipient mice followed by challenge infection as indicated. For OT-I cell adoptive transfers, OT-I cells were obtained from the blood or spleen and then stained with K^b/Ova tetramers to determine numbers of OT-I cells and then <5000 OT-I cells were transferred into recipient mice. Adoptive transfer experiments were done with either OTI-TRAF6$^{flx/flx}$CD4-cre(−) or OTI-TRAF6$^{flx/+}$CD4-cre (+) cells, and this confirmed that CD4-cre-expressing cells are not rejected.

In vitro T cell stimulation

Naïve T cells were activated with αCD3 (1.0μg/ml), αCD28 (0.5μg/ml), and 100U/ml of IL-2 for 3 or 4 days and then assayed as indicated.

Metabolism assays

All activated T cells were rested in the absence of IL-2 for 3–4 hours (rest period) prior to culturing in the absence or presence of IL-2 or glucose (withdrawal period). The glycolytic rate of T cells was determined by measuring the conversion of 5-^{3}H-glucose to tritiated water, as described previously [33]. Briefly, *in vitro* activated OT-I cells were plated at 1×10^6/ml in 24 well plates and cultured +/− glucose and +/− IL-2 100U/ml as indicated for 14 – 16 hrs. Cells were harvested, washed twice and resuspended in either glucose-free or glucose replete medium +/− 100u/ml of IL-2 (RPMI, Gibco), and then incubated with 10 μmCi of 5-^{3}H-glucose (Perkin-Elmer) at 37°C for 1 h. The reaction was stopped by adding HCl (0.1M final). ^3H_2O generated by enolase activity was separated from 5-^{3}H-glucose by diffusion, and counts were measured using a 1450 Microbeta scintillation counter (Wallac). Measurement of mitochondrial-dependent β-oxidation of fatty acids was conducted as previously described with modifications [34]. In brief, 1×10^6 activated OT-I cells were cultured +/− glucose and/or +/− IL-2 100U/ml as indicated for 14 – 16 hrs. [9,10-^{3}H]-palmitic acid complexed to BSA (essentially fatty acid free; Sigma) was added to the cultures and incubated for 6–8 hours. Mitochondrial-independent β-oxidation was assessed by measuring [9,10-^{3}H]-palmitate oxidation in the presence of 200 μM etomoxir (Sigma), an irreversible inhibitor of carnitine palmitoyltransferase I (CPT1), the rate-limiting enzyme for mitochondrial import of long-chain fatty acids. Supernatant was applied to ion-exchange columns (Dowex 1X8–200, Sigma), and ^3H_2O recovered by eluting the columns with water. One-fifth of the recovered ^3H_2O was then used for scintillation counting. The rate of β-oxidation was calculated as the difference between oxidation counts in the presence or absence of etomoxir, and expressed as CPM per 1×10^6 cells. Metformin (2mM) [35] or triciribine (1μM) 36 was added during the IL-2 withdrawal period as indicated.

In vivo drug treatment

Mice were injected daily with 300ul of PBS or metformin (250mgxkg) [35] in 300ul of PBS. Rapamycin was dissolved in PBS / 5% DMSO and injected daily (1.5mg/kg) 37. The PBS vehicle for these experiments also contained 5% DMSO. No effect between PBS and PBS / 5% DMSO was detected.

Microarray

Following OT-I cell adoptive transfer and LmOva infection, splenocytes and blood were harvested (at d6 and d10 post-infection) from individual mice and donor cells were sorted (FACS Vantage, BD bioscience) on the CD45.2 donor marker directly into Trizol LS (Invitrogen). RNA was extracted and samples were analyzed using the Affymetrix Mouse Genome 430 2.0 Array at the University of Pennsylvania Microarray Core Facility. We first used the gcrma package [38] from the Bioconductor software 39 to generate $\log_2$ probesets expression levels. Hierarchical clustering showed one of the samples is an outlier and is excluded in subsequent analyses. We used the limma software package [40] from Bioconductor to assess the effect of time (d6 and d10) and genotype (WT and TRAF6$^{-/-}$) by fitting the expression levels of each probeset *i* using R model specification "expr ~ genotype * timepoint", which translates to the following model:

$$x_{ij}=m_i+a_iG_{ij}+b_iT_{ij}+r_iGT_{ij}+e_{ij}$$

where x_{ij} is the $\log_2$ expression level in sample j, m_i is the overall mean $\log_2$ expression level, G_{ij} is the indicator variable whether sample j is TRAF6$^{-/-}$ (G_{ij}=1 if sample j is TRAF6$^{-/-}$, 0 otherwise), T_{ij} is the indicator variable whether sample j is harvested at d10, and GT_{ij} is the genotype-timepoint interaction term (GT_{ij} = 1 if and only if G_{ij}=1 and T_{ij}=1), a_i, b_i, and r_i are the coefficients of the genotype and timepoint effects to be estimated, and e_{ij} is the normally-distributed error term. We determined whether probesets are differentially expressed between genotypes at d6 (d10) using the classifyTestsF function (nested F-test) from limma with default p-value cutoff 0.01 and generated Venn diagrams.

Western blot analysis

Cell lysate preparation, SDS-PAGE, electrophoretic transfer, immunoblotting, and development using enhanced chemiluminescence were accomplished as previously described [41]. To isolate *ex vivo* T_E, OT-I cells were adoptively transferred into CD45.1 congenic mice followed by LmOva infection. At d7 post-infection donor cells were isolated (at 4°C) by MACS purification (Miltenyi Biotech). All antibodies for western analysis were purchased from Cell Signaling. P-AMPK measures phosphorylation at Thr-172.

Acknowledgments

We thank Connie Krawczyk, Carolyn King, Michael Farrar, Yvonne Paterson, Zhen-Kun Pan, and Edward J. Pearce. This work is supported in part by grants from the NIH (Y.C.; H.S.), CIHR (R.G.J.), and an NCI Institutional Training Grant (E.L.P).

References

1. Harty JT, Badovinac VP. Shaping and reshaping CD8+ T-cell memory. Nat Rev Immunol 2008;8:107–119. [PubMed: 18219309]
2. Prlic M, Williams MA, Bevan MJ. Requirements for CD8 T-cell priming, memory generation and maintenance. Curr Opin Immunol 2007;19:315–319. [PubMed: 17433873]
3. Lanzavecchia A, Sallusto F. Progressive differentiation and selection of the fittest in the immune response. Nat Rev Immunol 2002;2:982–987. [PubMed: 12461571]

4. King CG, et al. TRAF6 is a T cell-intrinsic negative regulator required for the maintenance of immune homeostasis. Nat Med 2006;12:1088–1092. [PubMed: 16921377]
5. Bachmaier K, et al. Negative regulation of lymphocyte activation and autoimmunity by the molecular adaptor Cbl-b. Nature 2000;403:211–216. [PubMed: 10646608]
6. Shedlock DJ, Shen H. Requirement for CD4 T cell help in generating functional CD8 T cell memory. Science 2003;300:337–339. [PubMed: 12690201]
7. Sun JC, Bevan MJ. Defective CD8 T cell memory following acute infection without CD4 T cell help. Science 2003;300:339–342. [PubMed: 12690202]
8. Janssen EM, et al. CD4+ T cells are required for secondary expansion and memory in CD8+ T lymphocytes. Nature 2003;421:852–856. [PubMed: 12594515]
9. Badovinac VP, Haring JS, Harty JT. Initial T cell receptor transgenic cell precursor frequency dictates critical aspects of the CD8(+) T cell response to infection. Immunity 2007;26:827–841. [PubMed: 17555991]
10. Joshi NS, et al. Inflammation directs memory precursor and short-lived effector CD8(+) T cell fates via the graded expression of T-bet transcription factor. Immunity 2007;27:281–295. [PubMed: 17723218]
11. Kaech SM, et al. Selective expression of the interleukin 7 receptor identifies effector CD8 T cells that give rise to long-lived memory cells. Nat Immunol 2003;4:1191–1198. [PubMed: 14625547]
12. Schluns KS, Williams K, Ma A, Zheng XX, Lefrancois L. Cutting edge: requirement for IL-15 in the generation of primary and memory antigen-specific CD8 T cells. J Immunol 2002;168:4827–4831. [PubMed: 11994430]
13. Schluns KS, Kieper WC, Jameson SC, Lefrancois L. Interleukin-7 mediates the homeostasis of naive and memory CD8 T cells in vivo. Nat Immunol 2000;1:426–432. [PubMed: 11062503]
14. Tan JT, et al. Interleukin (IL)-15 and IL-7 jointly regulate homeostatic proliferation of memory phenotype CD8+ cells but are not required for memory phenotype CD4+ cells. J Exp Med 2002;195:1523–1532. [PubMed: 12070280]
15. Surh CD, Boyman O, Purton JF, Sprent J. Homeostasis of memory T cells. Immunol Rev 2006;211:154–163. [PubMed: 16824125]
16. Burchill MA, et al. Distinct effects of STAT5 activation on CD4+ and CD8+ T cell homeostasis: development of CD4+CD25+ regulatory T cells versus CD8+ memory T cells. J Immunol 2003;171:5853–5864. [PubMed: 14634095]
17. Kelly J, et al. A role for Stat5 in CD8+ T cell homeostasis. J Immunol 2003;170:210–217. [PubMed: 12496402]
18. Buzzai M, et al. The glucose dependence of Akt-transformed cells can be reversed by pharmacologic activation of fatty acid beta-oxidation. Oncogene 2005;24:4165–4173. [PubMed: 15806154]
19. Rathmell JC, Vander Heiden MG, Harris MH, Frauwirth KA, Thompson CB. In the absence of extrinsic signals, nutrient utilization by lymphocytes is insufficient to maintain either cell size or viability. Mol Cell 2000;6:683–692. [PubMed: 11030347]
20. Lum JJ, et al. Growth factor regulation of autophagy and cell survival in the absence of apoptosis. Cell 2005;120:237–248. [PubMed: 15680329]
21. Frauwirth KA, et al. The CD28 signaling pathway regulates glucose metabolism. Immunity 2002;16:769–777. [PubMed: 12121659]
22. Jones RG, et al. The proapoptotic factors Bax and Bak regulate T Cell proliferation through control of endoplasmic reticulum Ca(2+) homeostasis. Immunity 2007;27:268–280. [PubMed: 17692540]
23. Jones RG, Thompson CB. Revving the engine: signal transduction fuels T cell activation. Immunity 2007;27:173–178. [PubMed: 17723208]
24. Fox CJ, Hammerman PS, Thompson CB. Fuel feeds function: energy metabolism and the T-cell response. Nat Rev Immunol 2005;5:844–852. [PubMed: 16239903]
25. Buzzai M, et al. Systemic treatment with the antidiabetic drug metformin selectively impairs p53-deficient tumor cell growth. Cancer Res 2007;67:6745–6752. [PubMed: 17638885]
26. Sipula IJ, Brown NF, Perdomo G. Rapamycin-mediated inhibition of mammalian target of rapamycin in skeletal muscle cells reduces glucose utilization and increases fatty acid oxidation. Metabolism 2006;55:1637–1644. [PubMed: 17142137]

27. Peng T, Golub TR, Sabatini DM. The immunosuppressant rapamycin mimics a starvation-like signal distinct from amino acid and glucose deprivation. Mol Cell Biol 2002;22:5575–5584. [PubMed: 12101249]

28. Brown NF, Stefanovic-Racic M, Sipula IJ, Perdomo G. The mammalian target of rapamycin regulates lipid metabolism in primary cultures of rat hepatocytes. Metabolism 2007;56:1500–1507. [PubMed: 17950100]

29. Moore MW, Carbone FR, Bevan MJ. Introduction of soluble protein into the class I pathway of antigen processing and presentation. Cell 1988;54:777–785. [PubMed: 3261634]

30. Huang X, et al. Important role of the LKB1-AMPK pathway in suppressing tumorigenesis in PTEN-deficient mice. Biochem J 2008;412:211–221. [PubMed: 18387000]

31. Pearce EL, Shen H. Generation of CD8 T cell memory is regulated by IL-12. J Immunol 2007;179 (4):2074. [PubMed: 17675465]

32. Foulds KE, et al. Cutting edge: CD4 and CD8 T cells are intrinsically different in their proliferative responses. J Immunol 2002;168(4):1528. [PubMed: 11823476]

33. Elstrom RL, et al. Akt stimulates aerobic glycolysis in cancer cells. Cancer Res 2004;64(11):3892. [PubMed: 15172999]

34. Deberardinis RJ, Lum JJ, Thompson CB. Phosphatidylinositol 3- kinase-dependent modulation of carnitine palmitoyltransferase 1A expression regulates lipid metabolism during hematopoietic cell growth. J Biol Chem 2006;281(49):37372. [PubMed: 17030509]

35. Buzzai M, et al. Systemic treatment with the antidiabetic drug metformin selectively impairs p53-deficient tumor cell growth. Cancer Res 2007;67(14):6745. [PubMed: 17638885]

36. Karst AM, Dai DL, Cheng JQ, Li G. Role of p53 up-regulated modulator of apoptosis and phosphorylated Akt in melanoma cell growth, apoptosis, and patient survival. Cancer Res 2006;66 (18):9221. [PubMed: 16982766]

37. Albert MH, Yu XZ, Martin PJ, Anasetti C. Prevention of lethal acute GVHD with an agonistic CD28 antibody and rapamycin. Blood 2005;105(3):1355. [PubMed: 15459004]

38. Jean (ZHIJIN) Wu and Rafael Irizarry with contributions from James MacDonald Jeff Gentry. gcrma: Background Adjustment Using Sequence Information. 2008 R package version 2.12.1.

39. Gentleman RC, et al. Bioconductor: open software development for computational biology and bioinformatics. Genome Biol 2004;5(10):R80. [PubMed: 15461798]

40. Smyth, GK. Limma: linear models for microarray data. In: Gentleman, R.; Carey, V.; Dudoit, S.; Irizarry, R.; Huber, W., editors. 'Bioinformatics and Computational Biology Solutions using R and Bioconductor'. New York: Springer; 2005. p. 397-420.

41. Kobayashi T, et al. TRAF6 is a critical factor for dendritic cell maturation and development. Immunity 2003;19(3):353. [PubMed: 14499111]

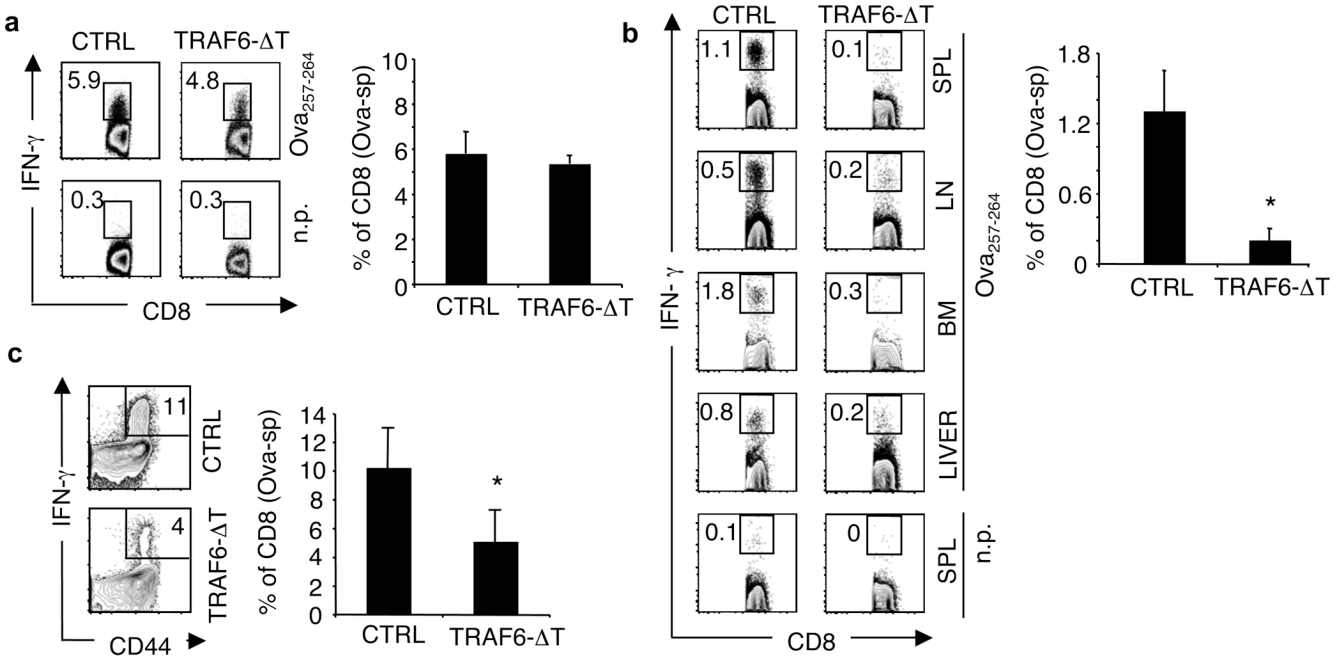

Figure 1. TRAF6-ΔT mice mount normal T_E responses, but have impaired T_M development following immunization with *L. monocytogenes*

Control (CTRL) and TRAF6-ΔT mice were LmOva-immunized and spleen (a and c) or spleen (SPL), lymph nodes (LN), and bone marrow (BM) cells (b) were Ova peptide-restimulated and analyzed for intracellular IFN-γ 7 days (a) (*n*=3–5 per group) or 60 days (*n*=3 per group) (b) post-infection. (c) 60 days post-immunization mice were challenged with LmOva and Ova-specific cells were analyzed 7 days post-challenge (*n*=3 per group). Dot plots and bar graphs show percentages of CD8 T cells producing IFN-γ (means ± standard deviation) *p=0.02 (b), 0.0005 (c).

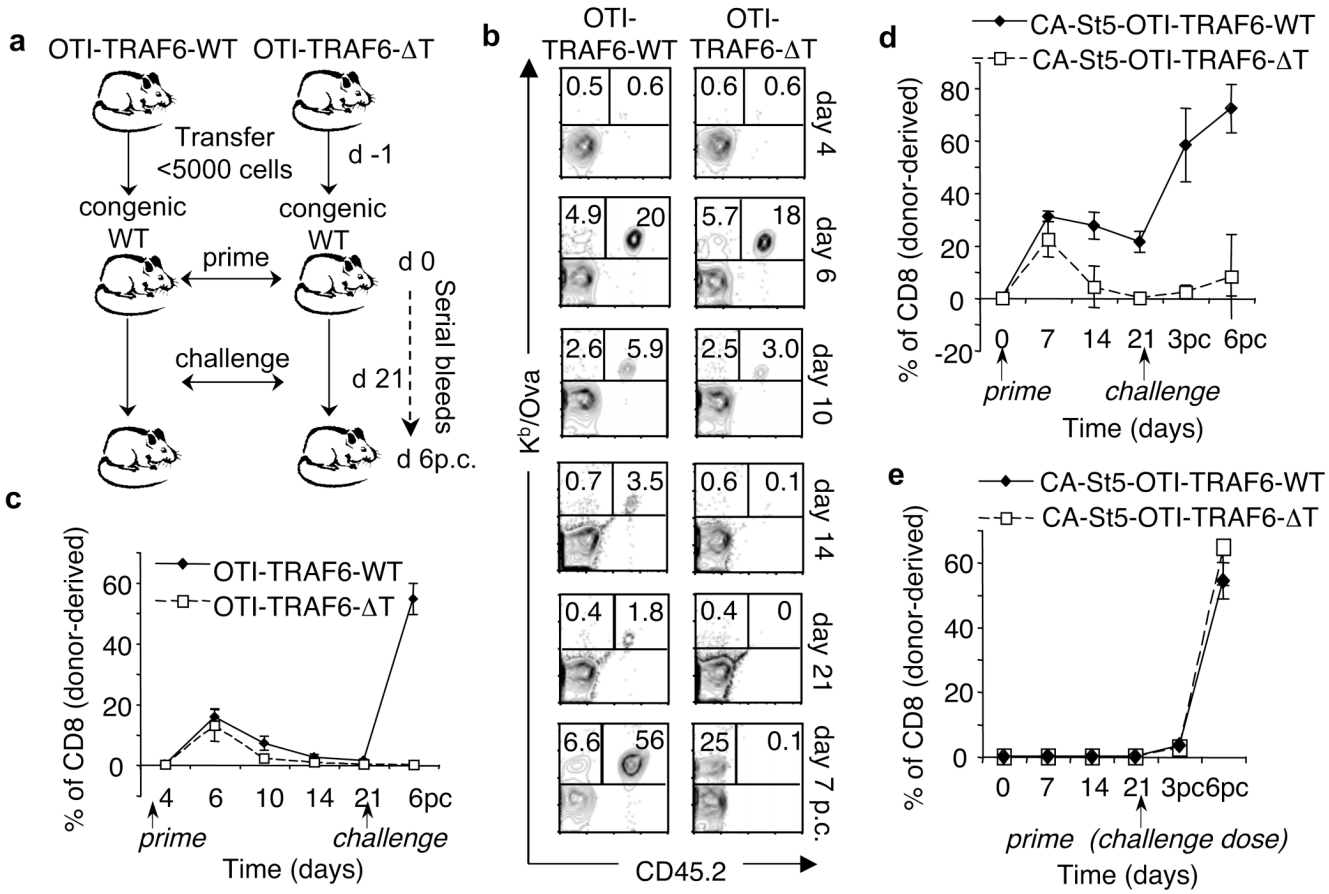

Figure 2. TRAF6 intrinsically regulates CD8 T_M generation

OT-I cells (<5000) from OTI-TRAF6-WT and OTI-TRAF6-ΔT (CD45.2) (a–c) or CA-St5-OTI-TRAF6-WT and CA-St5-OTI-TRAF6-ΔT mice (CD45.2) (d,e) were transferred into CD45.1 recipients (*n*=5–9 per group) and LmOva-immunized. Three weeks post-transfer immune (a–d) or unimmunized mice (e) were LmOva-challenged. Mice were bled as indicated and cells surface stained. Dot plots show donor cells by CD45.2 and K^b/Ova tetramer (numbers indicate total CD8 T cell percentages that are host- or donor-derived). Line graphs represent percentages of donor-derived CD8 T cells (means ± standard deviation).

a

Group	# of genes up or down	# KEGG genes	% of input	# of pathways
d6 up	39	8	20	0
d6 down	52	12	23	0
d10 up	38	6	15	0
d10 down	54	12	22	3

KEGG pathway	# of genes	% of input	P-value
Valine, leucine and isoleucine degradation	3	5.6	0.0044
Fatty acid metabolism	3	5.6	0.0046
Bile acid biosynthesis	2	3.7	0.078

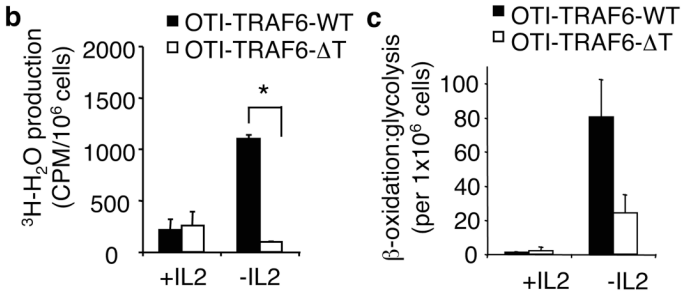

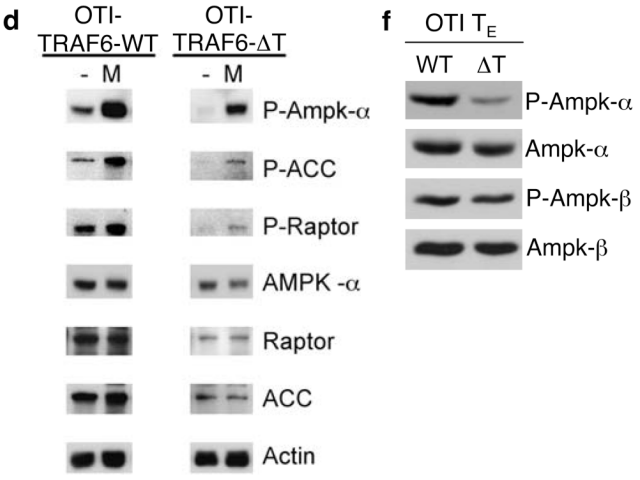

Figure 3. TRAF6-deficient CD8 T cells display defects in fatty acid metabolism that can be corrected by metformin

OT-I cells (<5000) from OTI-TRAF6-WT and OTI-TRAF6-ΔT mice (CD45.2) were transferred into CD45.1 recipients and immunized with LmOva. 6 (*n*= 3 per group) and 10 (*n*=5 per group) days post-infection donor cells were analyzed by microarray (a and SI Fig. 17). Tables generated using NIAID DAVID and KEGG databases (a). FAO (measured as mitochondrial β-oxidation) of activated OTI-TRAF6-WT and OTI-TRAF6-ΔT cells post-IL-2 withdrawal, *p value=0.012 (b). Ratio of β-oxidation to glycolysis in activated OTI-TRAF6-WT and OTI-TRAF6-ΔT cells post-IL-2 withdrawal (c). Western analysis of cells 16 hours post-IL-2 withdrawal +/− metformin (Acetyl CoA carboxylase (ACC) and Raptor are examined as targets of AMPK) (d). Mitochondrial β-oxidation of activated OTI-TRAF6-WT and OTI-TRAF6-ΔT cells +/− IL-2, where cells received nothing (−), triciribine (T), or metformin (M) for 16 hours, *p value = 0.003 (e). Western analysis of purified OTI-TRAF6-WT and OTI-TRAF6-ΔT T_E donor cells (7 days post-infection) (f).

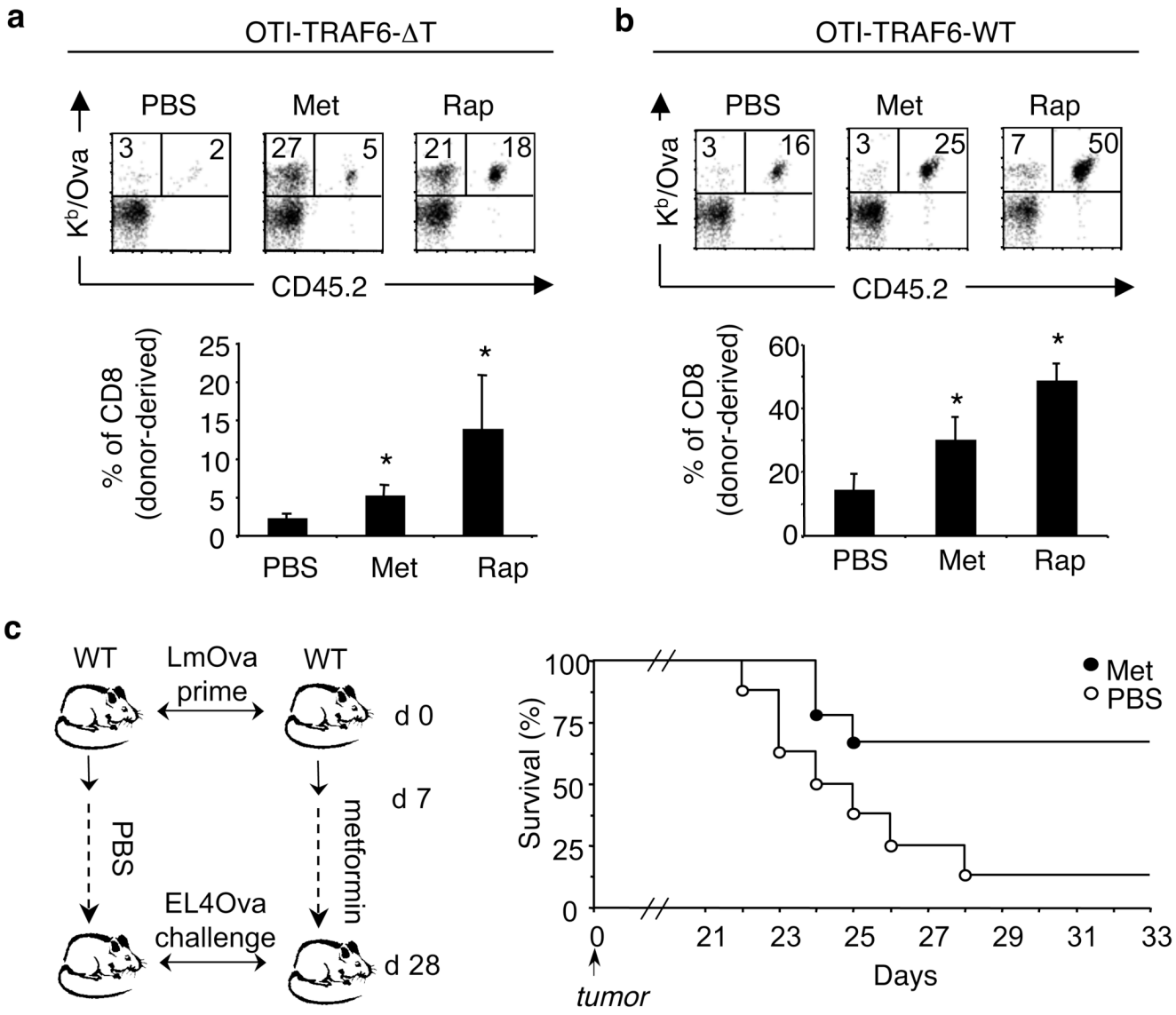

Figure 4. Metformin treatment promotes T_M generation and protective immunity following infection and tumor challenge

(a,b) OT-I cells (<5000) from OTI-TRAF6-WT and OTI-TRAF6-ΔT mice (CD45.2) were transferred into CD45.1 recipients and immunized with LmOva. 8 days post-infection mice were injected daily with PBS (*n*=7–9 per group), metformin (*n*=7–9 per group), or rapamycin (*n*=5 per group) for three weeks and were then challenged with LmOva. Ova-specific responses of host and donor cells in the blood were measured 5 days post-challenge. Dot plot numbers reflect the percentages of total CD8 T cells that are host or donor-derived (Ova-specific). Bar graphs represent percent of CD8 T cells that are donor-derived (means ± standard error). *p values (comparing to PBS) = 0.015 (Met) and 0.000038 (Rap)(a), 0.0373 (Met) and 0.00028 (Rap)(b). (c) C57BL/6 mice were immunized and daily injections of metformin or PBS began 7 days post-infection. Three weeks later treatments ceased and mice were inoculated with EL4-Ova tumors. Tumors became palpable by 18 days post-inoculation and mice were euthanized when tumors reached 2cm. Graph reflects percent survival (*n*=9, metformin and *n*=8, PBS).